LA--10029-MS

DE84 013861

Thermal Instabilities in the Edge Region of Reversed-Field Pinches

J. Goedert*
J. P. Mondt

DISCLAIMER

*Federal University of Rio Grande do Sul, Porto Alegre, Brazil.

Los Alamos National Laboratory
Los Alamos, New Mexico 87545

THERMAL INSTABILITIES IN THE EDGE REGION OF REVERSED-FIELD PINCHES

by

J. Goedert and J. P. Mondt

ABSTRACT

Thermal stability of the edge region of reversed-field pinch configurations is analyzed within the context of a two-fluid model. Two major sources of instability are identified in combination with a parallel electric field: either an electron temperature gradient and/or a density gradient that leads to rapid growth (of several to many ohmic heating rates) over a region of several millimeters around the mode-rational surfaces in the edge region. The basic signature of both instabilities is electrostatic. In the case of the density gradient mode, the signature relies on the effects of electron compressibility, whereas the temperature gradient mode can be identified as the current-convective instability by taking the limit of zero diamagnetic drift, density gradient, thermal force, drift heat flux, and electron compressibility.

INTRODUCTION

The effects of longitudinal currents on plasma stability are known to be essential in confinement studies of tokamaks.[1-3] Recently, application of the theory of reconnection to the case of reversed-field pinches was shown to predict the occurrence of double-tearing modes,[4] with possible implications for the interpretation of dynamo action, although only for sufficiently low

temperatures in the plasma core. The subject of this investigation into the nature of current-driven instabilities has a somewhat different motivation and focus; it addresses the influence of longitudinal current on the existence of a turbulent region in the plasma edge in reversed-field pinches during the first millisecond or so after burn-through, during which time the electron edge temperature is presumably low enough to imply a rather high resistive dissipation rate. Such high dissipation rates mandate a careful examination of the electron energy balance of the time-dependent state, and, thereby, the inclusion of rapid instabilities of the thermal type. It should be recalled here that turbulence, through the enhanced losses associated with it, is especially dangerous in the edge region because of the proximity of the wall.

Current-convective[5] instability has been clearly identified in earlier work under certain restrictive circumstances not applicable in the regime of interest to the edge region of reversed-field pinches. This type of instability was shown to give rise to enhanced thermal convection in the unstable region of the plasma column. The general aim of this work is to carry out an analysis of thermal stability applicable to conditions relevant to the edge region of reversed-field pinches.

The present thermal stability analysis has to be distinguished from some earlier treatments[3,6,7] that pertain to a regime of higher electron temperature. In particular, for edge temperatures on the order of 10 eV, it cannot be assumed that the parallel electron thermal conductivity is large enough to preclude longitudinal gradients; nor is there a competition between ohmic heating and perpendicular conductivity rates, as the latter are indeed negligible. The evolution of the instabilities typically takes place within several tens to several hundreds of microseconds, rather than on transport time scales. Because of these fast growth rates, the anomalous contributions to the transport coefficients are neglected. Consequently, the instabilities of interest fall into the general class of dissipative hydromagnetic instabilities, which are most simply treated by a classical two-fluid model.[8] This model is fairly realistic under the present circumstances, except for the neglect of finite ion Larmor radius effects. Inclusion of these effects would require a major increase in complication and intransparency, whereas, as shown in the subsequent sections, the basic physics of the presently investigated instabilities only depend on the electrons.

Because we expect the longitudinal gradients of the disturbances to be small (but finite), we will also investigate electromagnetic effects. Such effects may be important if the parallel electron drift approaches the Alfvén velocity. But because the basic instabilities are electrostatic in origin and the plasma beta in the edge region of reversed-field pinches is only about a percent or less, it is both illustrative and meaningful to start our presentation with the electrostatic model. Furthermore, because the eigenfrequencies are expected to be small compared with the Alfvén frequency ($|\omega|^2 << \omega_A^2$) over most of the domain of instability, inertial and viscous effects will be neglected in the perpendicular ion force balance. Because of the high parallel ion viscosity, it will be assumed that the parallel current disturbance is carried entirely by the electrons. Although the ohmic heating rate is rather high, it is typically equalled or exceeded by the parallel electron drift. Therefore, the model equations adopted in an earlier treatment[5] have to be modified to include the effects of electron pressure gradient and thermal force on the electron force balance. Furthermore, because the perpendicular drift frequencies may be of the same order or greater than the parallel electron drift frequency due to the flute-like structure of the instabilities ($k_\parallel << k_\perp$), the drift heat flux is kept in the electron energy balance. The contribution to the heat flow resulting from the relative drift between the species is also kept, unlike in earlier work.[5] In the electron energy equation, this contribution to the heat flow cancels the effect of the parallel thermal force on the perturbation in the electron temperature, but only in the electrostatic approximation and only in the energy balance, not in the parallel electron force balance. Moreover, in view of the inhomogeneity in the magnetic field profile in the edge region of reversed-field pinches, the effects of electron compressibility are maintained not only in the electron continuity equation but also in the electron energy balance. As will be shown, the effect of electron compressibility on the electron energy balance leads to a new source of instability, which consists of a combination of parallel current and density gradient.

We restrict ourselves to low beta by neglecting the contribution to the ohmic heating from the diamagnetic currents ($J_\perp^2 << J_\parallel^2$) and to low electron temperature by neglecting the contribution to the heat flow from the perpendicular electron thermal conductivity ($\omega_{ce}^2 \tau_c^2 >> k_\perp^2/k_\parallel^2$). We stress that the latter assumption also implies that anomalous contributions to the

perpendicular heat flow are not taken into account. This assumption is valid provided the edge temperature is low enough to justify the neglect on electron mobility due to field line wandering in the particular time scales of interest. In this respect it is sufficient to assume (1) that there are no anomalous contributions to the conductivity on the time scale of the linear growth, and (2) that the ratio of the radial excursion of field lines divided by the longitudinal distance travelled by them is less than the ratio of the parallel wave number divided by the perpendicular wave number. Despite the low value of plasma beta in the edge, effects due to perturbations in the magnitude of the magnetic field are retained in the electromagnetic treatment because of field curvature. The effects of field curvature on the equilibrium are included. However, Taylor-expanded profiles are used for the actual computations.

The present theory implicitly assumes the existence of a steady nonzero parallel electric field on the time scale of the linear growth. In a truly steady state, such a field must be excluded from the field-reversal layer (m = 0 modes), in view of Cowling's theorem.[9] However, the experimental data[10] indicate that a truly steady state is only of academic interest. Sustainment of field reversal requires a nonzero poloidal current density at the field-reversal layer. The long duration of this sustainment (several resistive diffusion times) has been the subject of various theoretical conjectures, in particular, the dynamo theory,[11,12] which relies on the nonlinear beating of magnetic field and kinetic disturbances to provide an additional mean field contribution to Ohm's law, as well as a recently proposed theory by Jacobson and Moses[13] that relies on a sufficient degree of field line stochasticity according to the model of Rechester and Rosenbluth.[14] This dynamo theory also relies on the fact that, for the observed plasma temperatures in its core, only a global Ohm's law exists because of the very long mean free paths for electrons (several hundred meters). The present theory assumes, but does not attempt to explain, the existence of a steady electric field (steady on the time scale of the linear growth, i.e., a fraction of an ohmic heating time). It is, furthermore, based only on the existence of a local Ohm's law in the edge region, where temperatures of about 10 eV would imply mean free paths of only several tens of centimeters.

BASIC ASSUMPTIONS AND EQUATIONS

Throughout this work we assume that the electron mean free path is much shorter than the characteristic length over which the plasma parameters change. This statement pertains both to the background and to the perturbations and both to the direction along the magnetic field and the perpendicular to it. Furthermore, we restrict ourselves to the case where the electron gyromotion is faster than the collision rate:

$$\omega_{ce}\tau_e >> 1 \quad . \tag{1}$$

In this case, the perpendicular mean free path is effectively limited to the distance travelled between two subsequent collisions caused by the ∇B-drift. Because in the perturbed state this drift transports electrons to a region with a slightly different temperature, this distance is the effective electron mean free path in the perpendicular direction The conditions on gradient scale lengths for the validity of the assumption of a local Maxwellian distribution function, therefore, are

$$r_e\lambda << L_\perp^2 \tag{2}$$

and

$$\lambda << L_\parallel \quad , \tag{3}$$

where λ is the mean free path for electrons and L_j is the gradient scale length in the j-direction.

In addition, we assume that the time variation is slow compared to the electron collision time, so that

$$|\omega|\tau_e << 1 \quad . \tag{4}$$

Under the conditions of Inequalities (2)-(4), the method of successive approximations to the distribution function applies to the electron constituent in the plasma if the interplay between collisional effects and plasma waves is ignored (as will be done here to follow common practice rather than common

sense). For a full display of the equations governing the electron density, velocity, and temperature, see Braginskii.[8]

Because our main interest is in thermal instabilities with large but finite parallel conductivity damping, the following ordering is adopted:

$$\frac{1}{\omega_{ce}\tau_e} << \frac{k_\parallel^2}{k_\perp^2} << 1 \quad . \tag{5}$$

As a result of Inequality (5), the contribution to the thermal force from the perpendicular electron temperature gradient drift can be neglected in both the electron force balance and the electron energy balance.

In view of the Inequalities (1) and (4), $|\omega| << \omega_{ce}$, and in view of the smallness of the electron Larmor radius ($r_e << L_\perp$), electron polarization and gyroviscous drifts can be neglected in the electron force balance. In addition it will be assumed that the electron diamagnetic drift frequency is much lower than the electron collision frequency. As a result, the effect of viscosity can be consistently neglected in the electron force balance. In addition, if we assume that the perpendicular diamagnetic drift frequency $\omega_D \equiv v_{De}/L_\perp$ is sufficiently small ($\omega_D^2 << \nu_e|\omega|$), the effects of viscous dissipation in the electron energy balance may be neglected. Finally, electron-ion temperature equilibration is a slow process on the time scale of linear growth and, hence, will be neglected.

Therefore, the following equations for the electron particle number density, velocity, and temperature are obtained:

$$\frac{\partial n}{\partial t} + \nabla\cdot n\underset{\sim}{v}_e = 0 \quad , \tag{6}$$

where n is the particle number density (quasi neutrality assumed) and $\underset{\sim}{v}_e$ is the electron fluid velocity;

$$J_\parallel = \sigma_\parallel\left(E_\parallel + \underset{\sim}{h}\cdot\frac{\nabla P_e}{en} + \tau\underset{\sim}{h}\cdot\frac{\nabla T_e}{e}\right) \quad , \tag{7}$$

where e is minus the electron charge, $J_{\parallel}$ is the current density parallel to the magnetic field, $\sigma_{\parallel}$ is the parallel electrical conductivity, $E_{\parallel}$ is the parallel electric field, P_e and T_e are the electron pressure and temperature, respectively, $\tau = 0.71$ is a parameter that labels the terms proportional to the effects of thermal force and the contribution to the heat flow caused by the relative drift between the species, and $\underset{\sim}{h}$ is the unit vector along the magnetic field. Furthermore,

$$\underset{\sim}{v}_{e\perp} = c(\underset{\sim}{E} + \frac{\nabla P_e}{en}) \times \frac{\underset{\sim}{h}}{B} \tag{8}$$

and

$$\frac{\partial P_e}{\partial t} + \underset{\sim}{v}_e \cdot \nabla P_e + \frac{5}{3} P_e \nabla \cdot \underset{\sim}{v}_e = Q_e \quad , \tag{9}$$

where Q_e is the total source of the electron energy equation:

$$Q_e \equiv \frac{2}{3} \frac{J_{\parallel}^2}{\sigma_{\parallel}} + \varphi(T_e) + \frac{2}{3} \nabla \cdot (\chi_{\parallel}^e \underset{\sim}{hh} \cdot \nabla T_e) + \frac{5}{3} \nabla \cdot (\frac{cP_e}{eB} \underset{\sim}{h} \times \nabla T_e) + \frac{2}{3} \frac{\tau T_e}{e} \nabla \cdot \underset{\sim}{J}_{\parallel} \quad , \tag{10}$$

where $\chi_{\parallel}^e$ is the electron thermal conductivity along field lines. In Eq. (10), in addition to the ohmic heating and the parallel electron thermal conductivity, the drift heat flux and the combined contribution to the heat generated by the relative flow of the species and the parallel thermal force are included through the last two terms. In a steady state, Q_e vanishes by virtue of a balance between ohmic heating and the loss term $\varphi(T_e)$. For simplicity it is assumed that the total loss term responds instantly to the changes in the electron temperature during the linear growth time. Then, in the electrostatic approximation, φ can only be a function of electron temperature. Again for simplicity, we assume even for the electromagnetic case that the perturbations in ohmic heating rate and loss rate balance each other.

To a large extent the ion physics only weakly couple with the phenomena that give rise to the presently investigated thermal instabilities. This is especially true in the case of electrostatic waves, as will be demonstrated in the next section.

In view of the kinetic definition of the current density, the ion continuity equation is strictly satisfied as a result of the electron continuity equation in conjunction with Ampère's law, without displacement current (because the square of the plasma frequency is sufficiently large, i.e., $\omega_{pe}^2 >> |\omega|^2$, the displacement current can be neglected):

$$\underset{\sim}{J} = \frac{c}{4\pi} \nabla \times \underset{\sim}{B} \quad . \tag{11}$$

Because of the relatively long ion collision time, i.e., $\tau_i (k_\perp v_{th,i})^2 >> |\omega|$, the parallel ion viscosity dominates over inertial effects and may compete with the leading parallel ion forces. Under these circumstances, parallel viscosity provides a severe inhibition for parallel ion velocity perturbations. This consideration motivates our assumption that the parallel current is carried only by the electrons:

$$J_\parallel \simeq - e n v_{ed\parallel} \quad . \tag{12}$$

In the perpendicular direction the viscosity is limited by the magnetic field and the polarization and gyroviscous drifts are both neglected ($|\omega| << \omega_{ci}$, i.e., no finite Larmor effects). Therefore, they are not retained in the total perpendicular force balance:

$$\underset{\sim}{J}_\perp = c \frac{\underset{\sim}{h} \times \nabla P}{B} \quad . \tag{13}$$

Finally, nonadiabatic and compressibility effects in the ion energy equation are neglected completely:

$$\frac{\partial T_i}{\partial t} + \underset{\sim}{v}_i \cdot \nabla T_i = 0 \quad , \tag{14}$$

where $\underset{\sim}{v}_i$ is the ion fluid velocity. Because the only coupling between the electron temperature and the ion temperature is provided through the plasma force balance, ion temperature affects the thermal instabilities only through electromagnetic corrections. For the electrostatic case, Eq. (14) will not be needed, because total plasma force balance in that case is reduced to trivial expressions for the components of the magnetic field perturbations, the coefficients of which tend to zero.

ELECTROSTATIC STABILITY ANALYSIS

For electrostatic perturbations,

$$\delta \underset{\sim}{E} = -\nabla \delta\varphi \quad . \tag{15}$$

If we use the classical scaling for electrical conductivity,

$$\frac{\delta\sigma_{\parallel}}{\sigma_{\parallel}} = \frac{3}{2} \frac{\delta T_e}{T_e} \quad , \tag{16}$$

the parallel electron force balance [Eq. (7)] relates the electrostatic potential to electron pressure and temperature perturbations:

$$\delta\varphi = -\frac{3}{2} i \frac{E_{\parallel}}{k_{\parallel}} \frac{\delta T_e}{T_e} + \frac{P_e}{en} \frac{\delta P_e}{P_e} + \tau \frac{T_e}{e} \frac{\delta T_e}{T_e} \quad . \tag{17}$$

From the perpendicular electron force balance [Eqs. (8) and (17)], the radial component of the perturbed electron fluid velocity can be obtained explicitly in terms of the electron density and temperature perturbations:

$$\delta v_{er} = - U \frac{\delta T_e}{T_e} \quad , \tag{18}$$

where

$$U \equiv \frac{3}{2} c \frac{k_y}{k_\parallel} \frac{E_\parallel}{B} + i \tau V \quad , \tag{19}$$

with

$$V \equiv \frac{c k_y P_e}{e n B} \quad . \tag{20}$$

Here k_y is defined as the wave number perpendicular to the direction of the equilibrium magnetic field and the direction of the background gradients,

$$(\underset{\sim}{e}_\parallel \times \underset{\sim}{e}_r) \cdot \nabla = i k_y \quad , \tag{21}$$

when applied to a scalar perturbation, where $\underset{\sim}{e}_j$ denotes the unit vector in the j-direction. Similarly, the divergence of the electron fluid velocity can be expressed as follows:

$$\nabla \cdot \delta \underset{\sim}{v}_e = - i \omega_N \frac{\delta n}{n} + \omega_T \frac{\delta T_e}{T_e} \quad , \tag{22}$$

where

$$\omega_N \equiv k_\parallel v_{e\parallel} - V \frac{d \ell n T_e}{dr} \tag{23}$$

and

$$\omega_T \equiv \frac{4\pi\ U}{c\ k_y\ B}\ (k_\parallel J_\parallel - k_y J_y) - i\ V\ \frac{d\ell nn}{dr} \quad . \tag{24}$$

Furthermore, as shown in the Appendix, the perturbation of the source term δQ_e in the electron energy balance equation [Eq. (9)] can be expressed in terms of the electron density and temperature perturbations as well:

$$\frac{\delta Q_e}{P_e} = Q_n\ \frac{\delta n}{n} + Q_T\ \frac{\delta T_e}{T_e} \quad , \tag{25}$$

where, for electrostatic pertubations,

$$Q_n = \frac{5}{3}\ i\ \zeta\ V\ \frac{d\ell nT_e}{dr} \tag{26}$$

and

$$Q_T = -\ \omega_{CD} + \frac{5}{3}\ i\ \zeta\ V\ \frac{d\ell nB}{dr} \quad , \tag{27}$$

with $\omega_{CD} \equiv k_\parallel^2 \chi_\parallel^e / n$ as the electron thermal conductivity damping and $\zeta = 1$ as a label to indicate the contribution from the drift heat flux term in the electron energy equation. As pointed out before, in the electrostatic case the ion temperature does not couple to the electron temperature.

Substitution of Eqs. (18), (22), and (25) into the electron continuity equation and the electron energy balance equation yields two homogeneous algebraic relations between δn and δT_e. The resulting dispersion relation reads

$$\hat{\omega}^2 - i\hat{\omega}\ (Q_T + U\ \frac{d\ell nT_e}{dr} - \frac{2}{3}\ \omega_T - \ i\ \omega_N) + (U\ \frac{d\ell nn}{dr} - \omega_T)(Q_n + \frac{2}{3}\ i\ \omega_N) = 0 \quad , \tag{28}$$

where

$$\hat{\omega} = \omega - \underset{\sim}{k}\cdot\underset{\sim}{v}_e + \omega_N \quad . \tag{29}$$

We stress that this dispersion equation is valid for any mode-rational surface, provided the basic assumptions about the regime of interest for the edge region in reversed-field pinches are met. Two instabilities can be distinguished: (1) a current-convective branch with possibly positive growth that reproduces earlier results[5] when dn/dr = 0 in the absence of compressibility, electron pressure gradient, thermal force corrections to Ohm's law, and neglect of drift heat flux ($\zeta \to 0$), and (2) a different instability is identified by setting $dT_e/dr \to 0$. Then, the expression for the growth rate is found to be (for small $k_\parallel$)

$$\gamma = 4\pi \left(\frac{k_y J_y - k_\parallel J_\parallel}{k_\parallel B}\right) \frac{E_\parallel}{B} - \omega_{CD} \quad . \tag{30}$$

However, for values of $k_\parallel$ corresponding to the region of instability, the contributions from the density gradient to the growth rate are found to be predominant; in essence, this instability is driven by density gradient. This instability, which in the general case is driven by a combination of parallel and perpendicular drifts (electron current and density gradient), requires compressibility. The dependence of the growth rate on the position with respect to the mode-rational surface is illustrated in the odd numbered figures in Figs. 1-9 and in Figs. 8 and 10.

The instabilities are moderately localized, with typical growth rates of several to many ohmic heating rates. Although our theory applies to most of the domain of instability, we stress that near the mode-rational surface, electromagnetic effects cannot be ignored because of the absence of line-bending there. Electromagnetic effects will be discussed in the next section. Obviously the neglect of finite Larmor radius corrections is especially invalid in the immediate vicinity of the mode-rational surface, where the present continuum theory predicts a steep eigenfunction. In fact, the influence of the finite ion Larmor radius on the instabilities found in the present treatment is an entirely open question, since a typical value of an ion Larmor radius, which

is 1 or 2 mm, is not small compared to the gradient scale length of a typical growth rate profile. However, the presently studied instabilities are determined by electron physics rather than ion physics, as we have mentioned. Therefore, finite Larmor radius effects should perhaps be expected to be of the kind and magnitude encountered in the theory of tearing instabilities[15] (i.e., to be mild), rather than those encountered in the theory of such ion-pressure-driven modes as interchange instabilities.[16]

ELECTROMAGNETIC EFFECTS

In this section we investigate the influence of electromagnetic effects on the thermal instabilities identified in the electrostatic model. The electrostatic model predicts instability in a region over most of which inertial effects can be neglected, compared with line-bending:

$$|\omega|^2 << k_{\parallel}^2 V_A^2 \quad . \tag{31}$$

Clearly, inertial and electromagnetic corrections become important near the mode-rational surface where $k_{\parallel}$ tends to zero. However, in treating the electromagnetic effects, we strictly adhere to Inequality (31) by excluding a possibly nonzero region near the mode-rational surface where inertial effects have to be taken into account. As we will see, such a region typically is of the order of a thermal ion Larmor radius or narrower, and hence can only be treated correctly by a finite Larmor radius theory, which is beyond the scope of this report. However, despite the rather low values for plasma beta in the edge region, it is of interest to consider the effects of electromagnetic perturbations when the real part of the eigenfrequency can be comparable to the Alfvén frequency. This situation can occur for the thermal instabilities considered here because the parallel electron drift velocity is not very different in order of magnitude from the Alfvén frequency.

Because of the neglect of gyroviscous drifts in the perpendicular plasma force balance, Inequality (31) implies that only cross-field and diamagnetic drifts contribute to perpendicular force balance (the cross-field contributions cancel):

$$\delta \underset{\sim}{J}_{\perp} = c\, \delta\left(\frac{\underset{\sim}{h} \times \nabla P}{B}\right) \quad , \tag{32}$$

where P is the total kinetic pressure.

For simplicity, we assume that the ion temperature perturbation is not only unimportant in the electrostatic case but also in the electromagnetic case because our primary motivation for investigating electromagnetic effects is the possibility of a resonance between the electron drift and the Alfvén velocity. (For electrostatic perturbations ion temperature was shown to be unimportant for the modes studied; in the electromagnetic case, however, this is not clear beforehand unless $T_i << T_e$.) Therefore, the ion pressure perturbation is assumed to be due entirely to density perturbations:

$$\delta P_i = T_i\, \delta n \quad . \tag{33}$$

In addition to the electron continuity equation [Eq. (6)]; the perpendicular electron force balance incorporating only the cross-field and diamagnetic drifts [Eq. (8)]; the parallel electron force balance including resistive drag, electron pressure, and thermal force effects [Eq. (7)]; the electron energy balance [Eq. (9)] retaining electron compressibility, parallel thermal conductivity and ohmic heating, drift heat flux, parallel thermal force effects, and the contribution to the heat flow from the relative parallel drift; the quasi neutrality assumption; the assumption of high parallel ion viscosity [Eq. (12)]; and Ampère's law [Eq. (11)], we impose Faraday's law:

$$\frac{\partial \underset{\sim}{B}}{\partial t} = - c\, \nabla \times \underset{\sim}{E} \quad . \tag{34}$$

For simplicity we restrict considerations to modes with high radial wave numbers:

$$k_r \lambda_r >> 1 \quad , \tag{35}$$

where λ_r is the radial gradient scale length of the eigenfunction.

From the total plasma force balance [Eq. (13)], the radial and y-component of the current density perturbation can be expressed in terms of magnetic field and total kinetic pressure perturbations. Substitution of these expressions into Ampère's law and use of the flux law $\nabla . \underset{\sim}{B} = 0$ yield explicit expressions for the components of $\delta\underset{\sim}{B}$ in terms of δP:

$$\delta B_s = 4\pi \, Z_s \, \frac{\delta P}{B} \quad , \tag{36}$$

where s = r, y, ∥ and

$$Z_r = Z_o\left(k_\parallel^2 \, k_r - i \, k_y k_\parallel \, \frac{1}{B} \, \frac{dB_z}{dr} + i \, k_y^2 \, \frac{d\ell nB}{dr}\right) \quad , \tag{37}$$

$$Z_y = Z_o\left(k_\parallel^2 \, k_y + i \, k_r k_y \, \frac{1}{B} \, \frac{dB_z}{dr} - i \, k_r \, k_\parallel \, \frac{d\ell nB}{dr}\right) \quad , \tag{38}$$

and

$$Z_\parallel = -Z_o \, k_\parallel k_\perp^2 \quad , \tag{39}$$

with

$$Z_o = \left(k_\parallel\left[k_\perp^2 - i \, k_r \, \frac{d\ell nB}{dr} - \left(\frac{1}{B} \, \frac{dB_z}{dr}\right)^2\right] + \frac{k_y}{B} \, \frac{d\ell nB}{dr} \, \frac{dB_z}{dr}\right)^{-1} \quad . \tag{40}$$

Ampère's law and the flux law now yield explicit expressions for the current density perturbations:

$$\delta J_r = \left(4\pi\ J_\parallel\ Z_r - i\ c\ k_y\ B\right) \frac{\delta P}{B^2} \quad , \tag{41}$$

$$\delta J_y = \left(4\pi\ J_\parallel\ Z_y - 4\pi\ J_y\ Z_\parallel + i\ c\ k_r\ B\right) \frac{\delta P}{B^2} \quad , \tag{42}$$

and

$$\delta J_\parallel = 4\pi\ \frac{\underset{\sim}{k}\cdot\underset{\sim}{J}}{k_\parallel}\ Z_\parallel\ \frac{\delta P}{B^2} \quad . \tag{43}$$

We stress the regularity of these expressions in the limit when $k_\parallel$ tends to zero [Eq. (39)].

In view of Eqs. (36)-(43), the parallel electron force balance equation yields $\delta E_\parallel$ in terms of $\delta\sigma_\parallel$, δP, δP_e, and δT_e. By making use of the classical scaling law [Eq. (16)] and the relation between δP, δP_e, and δn implied by Eq. (33), $\delta E_\parallel$ can be expressed explicitly in terms of δn and δP_e alone:

$$\frac{\delta E_\parallel}{E_\parallel} = E_p\ \frac{\delta P_e}{P_e} + E_n\ \frac{\delta n}{n} \quad , \tag{44}$$

where

$$E_p = -\frac{3}{2} + (1+\tau)\ \frac{i\ k_\parallel\ P_e}{e\ n\ E_\parallel} + \beta_e\ E_o \tag{45}$$

and

$$E_n = \frac{3}{2} + \tau \frac{i\, k_\parallel\, P_e}{e\, n\, E_\parallel} + \beta_i\, E_o \quad , \tag{46}$$

with

$$E_o = \frac{1}{2}\left[\frac{\underset{\sim}{k}\cdot\underset{\sim}{J}}{k_\parallel J_\parallel} Z_\parallel + \frac{J_y}{J_\parallel} Z_y - \frac{B}{e\, n\, c\, E_\parallel}\left(J_y + c\,\tau\,\frac{1}{B}\frac{dP_e}{dr}\right) Z_r\right] \quad .$$

Substitution of Eq. (44) for $\delta E_\parallel$ into the radial component of Faraday's law yields an expression for δE_y in terms of the fundamental perturbations δn and δP_e:

$$ck_\parallel \frac{\delta E_y}{E_\parallel} + \left(4\pi\omega \frac{Z_r P_e}{E_\parallel B} - ck_y E_p\right)\frac{\delta P_e}{P_e} + \left(4\pi\omega \frac{Z_r P_i}{E_\parallel B} - ck_y E_n\right)\frac{\delta n}{n} = 0 \quad . \tag{47}$$

Equation (47) is one of three equations relating δn, δP_e, and δE_y, the other two being the electron continuity and energy equations. In fact, by using the parallel and perpendicular electron force balance equations [Eqs. (7) and (8)] and the parallel component of Faraday's law (to eliminate δE_r), the radial component and the divergence of the electron fluid velocity can be expressed in terms of electromagnetic perturbations and δE_y, δP_e, and δn:

$$\delta v_{er} = v_\parallel \frac{\delta B_r}{B} - c\,\frac{E_\parallel}{B}\frac{\delta B_y}{B} + c\,\frac{E_\parallel}{B}\frac{\delta E_\parallel}{E_\parallel} + i\, V \frac{\delta P_e}{P_e} \tag{48}$$

and

$$\nabla\cdot\delta\underset{\sim}{v}_e = -\, i\,\omega_N \frac{\delta n}{n} + \omega_T \frac{\delta T_e}{T_e} + \left(ik_\parallel v_\parallel - 4\pi \frac{E_\parallel J_\parallel}{B^2}\right)\frac{\delta J_\parallel}{J_\parallel} + i\left(\omega - \underset{\sim}{k}\cdot\underset{\sim}{v}\right)\frac{\delta B_\parallel}{B} \quad . \tag{49}$$

Here, electromagnetic effects are considered only within the context of the local approximation. Use of Eqs. (36), (39), and (43) and substitution of Eqs. (48) and (49) into the linearized electron continuity equation [Eq. (6)] give the following relation between the perturbations δE_y, δn, and δP_e:

$$c \frac{E_\parallel}{B} \frac{d\ell nn}{dr} \frac{\delta E_y}{E_\parallel} + \left(i\omega + \frac{1}{2} i\beta_i Z_\parallel \omega + \Omega_n \right) \frac{\delta n}{n} + \left(\frac{1}{2} i\beta_e Z_\parallel \omega + \Omega_p \right) \frac{\delta P_e}{P_e} = 0 \quad , \tag{50}$$

where

$$\Omega_n = i \, \underset{\sim}{k} \cdot \underset{\sim}{v}_e + i \, \omega_N - \omega_T + \beta_i \, \Omega_o \tag{51}$$

and

$$\Omega_p = i \, V \frac{d\ell nn}{dr} + \omega_T + \beta_e \, \Omega_o \quad , \tag{52}$$

where Ω_o is defined by

$$\Omega_o = \frac{1}{2} \left(v_{e\parallel} Z_r - c \frac{E_\parallel}{B} Z_y \right) \frac{d\ell nn}{dr} - 2\pi \frac{E_\parallel Z_r}{k_\parallel B^2} \underset{\sim}{k} \cdot \underset{\sim}{J} \quad .$$

Finally, substitution of Eqs. (48) and (49) into the energy balance equation [Eq. (9)] after its linearization, and use of Eqs. (36) and (41)–(43), yields the following relation between δE_y, δn, and δP_e:

$$c \frac{E_\parallel}{B} \frac{d\ell nP_e}{dr} \frac{\delta E_y}{E_\parallel} - \left(i\omega - \frac{5}{6} i\beta_e Z_\parallel \omega + Q_p - W_p \right) \frac{\delta P_e}{P_e} + \left(\frac{5}{6} i\beta_i Z_\parallel \omega - Q_n + W_n \right) \frac{\delta n}{n} = 0 \quad , \tag{53}$$

where W_n and W_p are defined by

$$W_n = \frac{5}{3}\left(i\,\omega_N - \omega_T\right) + \beta_i\, W_o \tag{54}$$

and

$$W_p = i\,\underset{\sim}{k}\cdot\underset{\sim}{v}_e + i\,V\,\frac{d\ell nP_e}{dr} + \frac{5}{3}\,\omega_T + \beta_e\, W_o \quad , \tag{55}$$

with

$$W_o = \frac{1}{2}\left(v_{e\parallel} Z_r - c\,\frac{E_\parallel}{B}\,Z_y\right)\frac{d\ell nP_e}{dr} - \frac{5}{3}\,2\pi\,Z_\parallel\,\frac{E_\parallel}{k_\parallel B^2}\,\underset{\sim}{k}\cdot\underset{\sim}{J} \quad . \tag{56}$$

In Eq. (53), the quantities δQ_n and δQ_p are given by Eqs. (A5) and (A6) in the Appendix.

Equations (47), (50), and (53) constitute a set of three homogeneous linear algebraic relations between the fundamental perturbations δF_y, δn, and δP_e. After some straightforward algebra, and assuming a nonvanishing background density gradient, a quadratic dispersion relation can be written in the following form:

$$d_o + i d_1 \omega + d_2 \omega^2 = 0 \quad , \tag{57}$$

where the coefficients d_o, d_1 and d_2 are defined by

$$d_o = k_\parallel\left(\Omega_p Q_n - \Omega_p W_n - \Omega_n Q_p + \Omega_n W_p\right) + c\,k_y\,\frac{E_\parallel}{B}\left(E_p \psi_n - E_n \psi_p\right) \quad , \tag{58}$$

$$d_1 = k_\parallel(Q_p - W_p - \Omega_n) - c\, k_y \frac{E_\parallel}{B}\left(\frac{d\ell nP_e}{dr} E_p + \frac{d\ell nn}{dr} E_n\right) + \frac{1}{2}\left(\beta_e \xi_n - \beta_i \xi_p\right) \quad , \quad (59)$$

and

$$d_2 = -\, k_\parallel + \frac{1}{2}\beta_e\left(\frac{5}{3} k_\parallel Z_\parallel + i \frac{d\ell nP_e}{dr} Z_r\right) + \frac{1}{2}\beta_i\left(k_\parallel Z_\parallel + i \frac{d\ell nn}{dr} Z_r\right) \quad , \quad (60)$$

where the quantities ψ_n, ψ_p, ξ_n, and ξ_p are defined by

$$\psi_\nu \equiv \frac{d\ell nn}{dr}\left(2\, Q_\nu - W_\nu\right) + \frac{d\ell nT_e}{dr}\Omega_\nu \quad (61)$$

and

$$\xi_\nu \equiv k_\parallel Z_\parallel\left(Q_\nu - W_\nu + \frac{5}{3}\Omega_\nu\right) + i\, Z_r \psi_\nu + c\, k_y Z_\parallel \frac{E_\parallel}{B}\left(\frac{2}{3}\frac{d\ell nn}{dr} - \frac{d\ell nT_e}{dr}\right)E_\nu \quad . \quad (62)$$

As expected, Eq. (57) reduces to the nonlocal electrostatic dispersion relation [Eq. (28)] in the absence of electromagnetic effects, i.e., $\beta_j \to 0$, $j = i, e$.

NUMERICAL RESULTS

The numerical results for the growth rates depend sensitively on various parameters, in particular on the gradients of particle number density, electron and ion temperature, and both components of the magnetic field.

To illustrate the essential features of the instabilities that can be identified, we take a case with poloidal mode number $m = 0$, a density gradient of -3×10^{12} cm^{-2}, and a gradient of -0.5 eV/cm for both electron and ion temperatures. The gradient of the toroidal magnetic field component is taken to be -20 G/cm. The gradient of the poloidal field is taken to be -74 G/cm, to roughly compensate (low beta) the field line curvature correction to equilibrium force balance at a mode-rational surface near the wall.

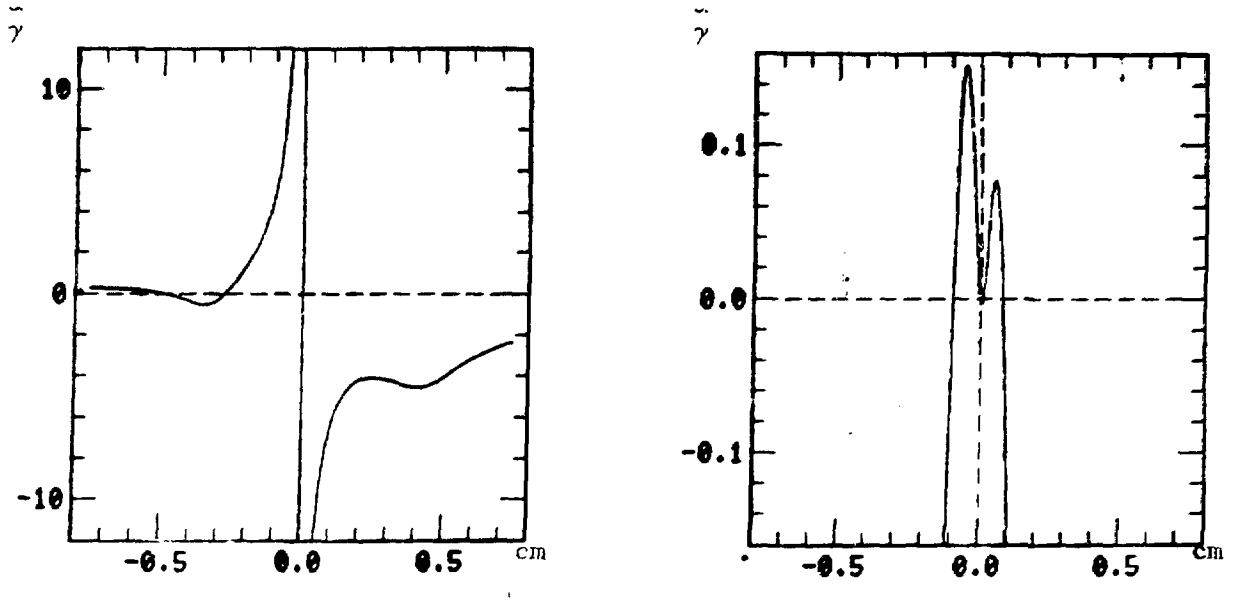

Fig. 1.

Nonlocal electrostatic growth rates in units of ohmic heating rate for both branches as a function of the distance to the mode-rational surface for poloidal mode number m = 0; B(0) = 1.5 kG, $B_\vartheta' = 74$ G/cm, $B_z' = -20$ G/cm, $n(0) = 1.5 \times 10^{13}/cm^3$, $n' = 0.3 \times 10^{13}/cm^2$, $T_e(0) = T_i(0) = 10$ eV, and $T_e' = T_i' = -0.5$ eV/cm.

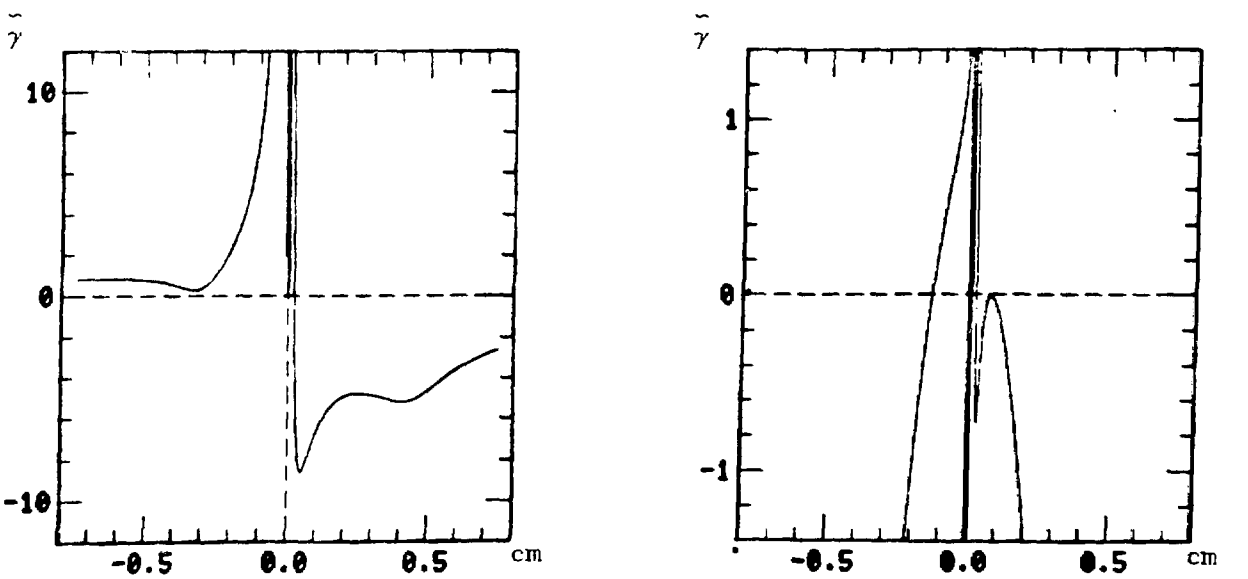

Fig. 2.

Same as in Fig. 1, but with electromagnetic corrections included in the local approximation.

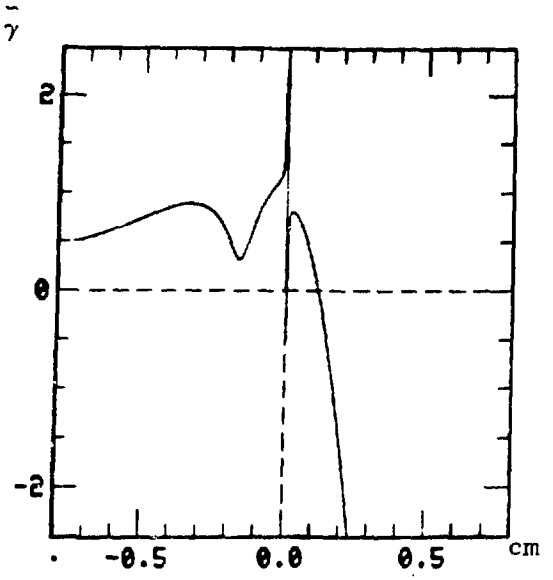

Fig. 3.

Relevant branch for nonlocal electrostatic growth rate; same as in Fig. 1, but with temperature gradients set to zero and $n' = -2 \times 10^{12} cm^{-2}$.

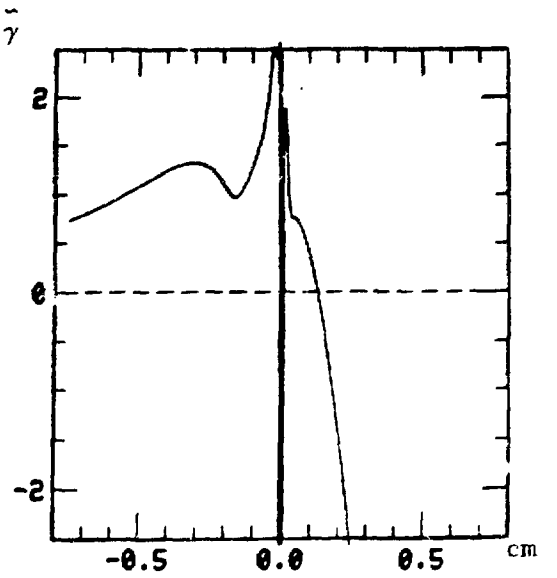

Fig. 4.

Same as Fig. 3, but with inclusion of electromagnetic effects in the local approximation.

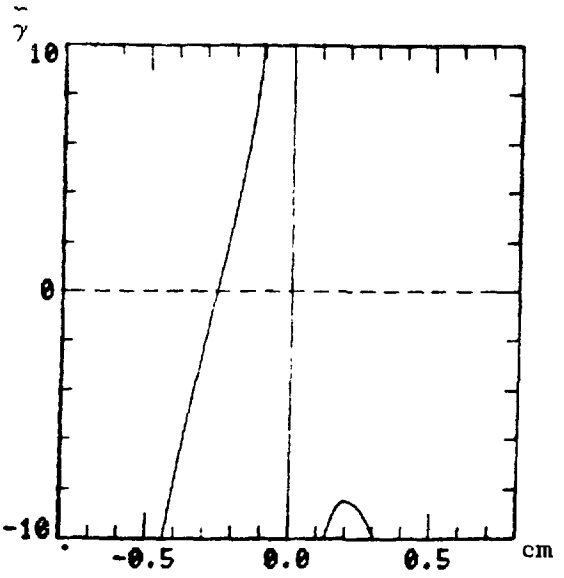

Fig. 5.

Same as Fig. 3, but $n' = 0$ and $T' = -1$ eV/cm for both electrons and ions.

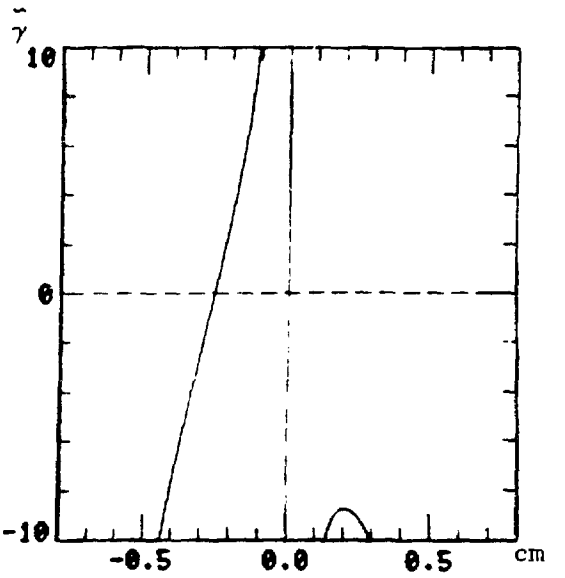

Fig. 6.

Same as Fig. 4, but $n' = 0$ and $T' = -1$ eV/cm for both species.

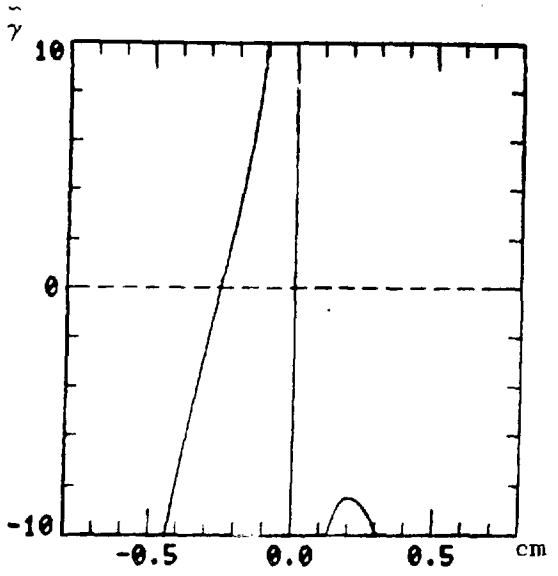

Fig. 7.

Same as Fig. 5, but without diamagnetic drift, thermal force, electron compressibility, and drift heat flux.

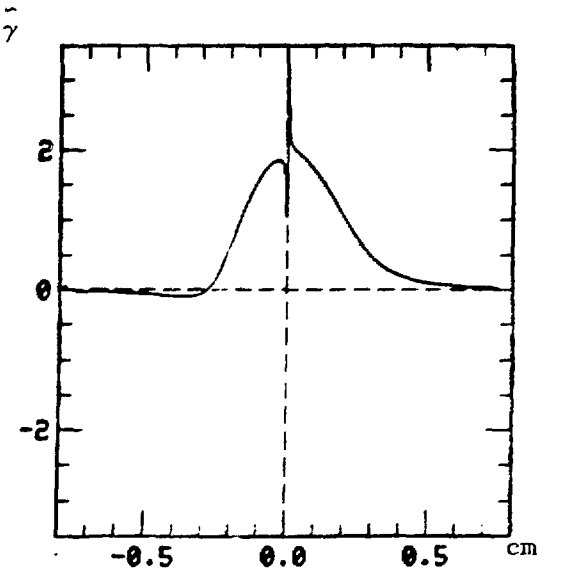

Fig. 8.

Same as Fig. 7 but without temperature gradients and for $n' = -2 \times 10^{12}/cm^2$.

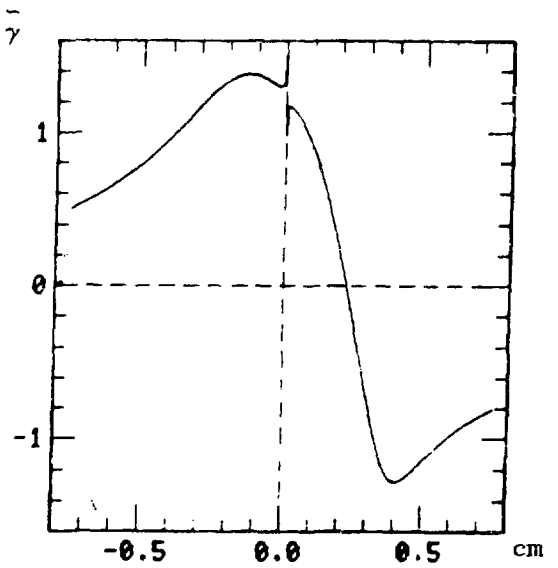

Fig. 9.

Same as in Fig. 3, but without heat drift flux.

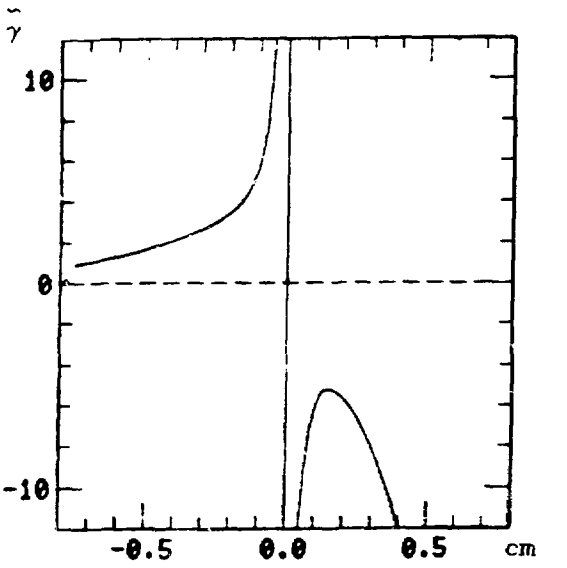

Fig. 10.

Same as Fig. 2 (left-hand side), but without heat drift flux.

For this case, Fig. 1 exemplifies the existence of a 3-mm-wide unstable region to the inside of the mode-rational surface for $T_e = T_i = 10$ eV, B = 1.5 kG, n = 1.5×10^{13} cm^{-3}, and $k_z = 1$ cm^{-1}. The radial mode number does not enter into the dispersion equation for this nonlocal, electrostatic case. Fig. 2 shows the same instability for the same parameters as Fig. 1, but with the inclusion of electromagnetic effects within the framework of a local analysis. For vanishing temperature gradients, a somewhat reduced growth rate persists over a somewhat wider region (Fig. 3). Again, the electromagnetic effects do not alter the basic signature of the instability (Fig. 4). However, density gradient was identified as an indispensable driving force for this instability. For nonzero negative temperature gradient but vanishing density gradient, another instability arises, both in the nonlocal electrostatic and in the electromagnetic cases (Figs. 5 and 6, respectively), and again exhibits instability over a region several millimeters wide. The growth rate of the current-convective instability violates the condition $|\omega|^2 << \omega_A^2$ in a region very close to the mode-rational surface not represented in the graphs. This instability can be identified as the current-convective instability and is not altered very much by the diamagnetic, thermal force, and compressibility effects incorporated in the present model (Fig. 7) However, these effects significantly modify the density gradient instability, as shown in Fig. 8; in particular, the region of instability is apparently narrowed by these additional effects, whereas the growth rate is also suppressed by them. Figures 9 and 10 show that the effect of the drift heat flux partly stabilizes the density gradient instability, but is of hardly any consequence to the current-convective instability.

CONCLUSIONS AND POSSIBLE IMPLICATIONS FOR REVERSED-FIELD PINCH OPERATION

We have investigated the thermal stability of reversed-field pinch configurations, with a special emphasis on the edge region, where the temperature presumably is low, at least in the first milliseconds of the discharge, whereas the current density can be large and cause fast thermal time scales.

On the basis of a two-fluid model that incorporates the effects of parallel resistivity, parallel thermal conductivity and ohmic heating, and electron drift heat flux and compressibility, as well as diamagnetic and parallel thermal force

effects, two main instabilities have been identified. They are both driven by a combination of parallel electric field and radial gradient. The electron temperature gradient drives an instability that can be identified as the current-convective instability[5] in the limit when the electron compressibility, drift heat flux, and diamagnetic and thermal force effects are being set equal to zero. The density gradient drives another instability, which relies on a proper treatment of the effects of electron compressibility. The growth rate for both instabilities is of the order of several ohmic heating rates over a region of a few millimeters around any mode-rational surface in the edge region (the only limitation here is the ordering of low electron temperature that excludes the interior). It should be mentioned, however, that the values found for the growth rates and the widths of the region of instability are highly sensitive to several parameters, i.e., magnetic field, temperature, density, and their gradients. Hence, a more comprehensive investigation will be needed eventually.

Furthermore, the reader is reminded once again of the a priori importance of finite ion Larmor radius effects, in view of the relatively narrow region of instability. Such importance may or may not be borne out by a finite Larmor radius theory, depending on whether or not the ion physics somehow is important enough for the presently investigated instabilities. Within the context of a fairly extensive two-fluid model, however, the present results were shown to be only weakly dependent upon the ion species.

The basic dispersion equations apply to any of the densely distributed mode-rational surfaces within the plasma edge region, with the same qualitative conclusions with regard to growth. Although a more detailed numerical scan of parameter space is required for any definitive conclusion, the present results indicate the possibility of overlap of regions of instability near adjacent mode-rational surfaces. In that case, the possibility for enhanced thermal convection in the entire edge region as a nonlinear consequence of the mode is indicated by the nonlinear analysis of the current-convective instability.[5] Admittedly, this analysis has to be redone for the conditions relevant to the edge region of reversed-field pinches. But the similarity between the present results for the temperature gradient mode and the simplest possible representation of the current-convective instability indicates the possibility that the nonlinear theory will essentially carry through as well. In that case, the net prediction of the classical theory of dissipative hydromagnetic

instabilities, as applied to the edge region of reversed-field pinches, is enhanced thermal loss through nonlinear thermal convection as a nonlinear consequence of thermal instabilities that arise because of the high parallel current density. In addition, any turbulence in the edge region may cause enhanced particle loss, because of the proximity of the wall. Therefore we speculate that the application of high ohmic currents in the first milliseconds or so after burn-through may lead to enhanced nonradiative losses, a speculation that may or may not have any bearing on recently found differences between the standard current wave form and a so-called ramped wave form,[17] in which the current was brought up more gradually after burn-through. In particular, the difference was mainly that the nonradiative losses in the ramped case were less than in the conventional mode of operation, whereas the total losses (radiative and nonradiative) were roughly equal.

ACKNOWLEDGMENTS

We are especially thankful for stimulating and helpful conversations with A. R. Jacobson, R. A. Gerwin, and D. A. Baker of the Los Alamos National Laboratory. We also thank the Los Alamos National Laboratory for its tbspitality during the course of this work, while J. Goedert was on leave of absence from the Federal University of Rio Grande do Sul, Porto Alegre, Brazil.

REFERENCES

1. H. P. Furth, J. Killeen, and M. N. Rosenbluth, Phys. Fluids 6, 459 (1963).

2. S. V. Mirnov and I. B. Semenov, in Plasma Physics and Controlled Nuclear Fusion Research (International Atomic Energy Agency, Austria, Vienna, 1971), Vol. II, p. 401.

3. E. J. Caramana and F. W. Perkins, Nucl. Fusion 21, 93 (1981).

4. E. J. Caramana, R. A. Nebel, and D. D. Schnack, Phys. Fluids 26, 1305 (1983).

5. B. B. Kadomtsev and O. P. Pogutse, in Reviews of Plasma Physics (Consultants Bureau, New York, 1970), Vol.5, pp. 249-400 (in particular, p. 293).

6. M. G. Haines and F. Marsh, J. Plasma Phys. 27, 427 (1982); A. Tomimura and G. Haines, J. Plasma Phys. 23, 1 (1980).

7. B. Coppi, Phys. Rev. Lett. 25, 851 (1970).

8. S. I. Braginskii, in Reviews of Plasma Physics (Consultants Bureau, New York, 1965), Vol. 1, p. 205.

9. T. G. Cowling, Mon. Not. R. Astron. Soc. (GB) 94, 39 (1933).

10. A. R. Jacobson, M. G. Rusbridge, and L. C. Burkhardt, "Polarized Radial Magnetic Fields and Outward Plasma Fluxes During Shallow Reversal Discharge in the ZT-40M Reversed-Field Pinch," Los Alamos National Laboratory document LA-UR-83-1541.

11. C. G. Gimblett and M. L. Watkins, in Controlled Fusion and Plasma Physics, Proc. 7th European Conf., Lausanne, (IAEA, Vienna, Austria, 1975)

12. L. Turner and J. P. Christiansen, Phys. Fluids 24, 983 (1981).

13. A. R. Jacobson and R. W. Moses, "Nonlocal dc Electrical Conductivity of a Lorentz Plasma in a Stochastic Magnetic Field," Los Alamos National Laboratory document LA-UR-83-3440, (to be published in Phys. Rev.).

14. A. B. Rechester and M. N. Rosenbluth, Phys. Rev. Lett. 40, 38 (1978).

15. E. Caramana, T. Cayton, R. Dagazian, D. Hewett, T. Hewitt, R. Lewis, J. Mondt, et al., "Dynamical Processes in the Reversed-Field Pinch," in Plasma Physics and Controlled Nuclear Fusion Research, (International Atomic Energy Agency, Vienna, Austria, 1983), Paper CN-41/H-2-2, pp. 597-606.

16. J. P. Mondt, Phys. Fluids 24, 1279 (1981).

17. J. A. Phillips, D. A. Baker, L. C. Burkhardt, R. Erickson, A. Haberstich, J. C. Ingraham, et al., "Observations of Ramped Current Operation in ZT-40M," Los Alamos National Laboratory report LA-10060-MS (May 1984).

APPENDIX

LINEARIZATION OF THE ENERGY EQUATION SOURCE TERMS.

The perturbed expression of Eq. (10) can be cast into the form of Eq. (25) by expanding each of its terms and making systematic use of the classical scaling law, Eqs. (36)-(40), (43), and the assumption that $J_{\|}$ and $\chi^{e}_{\|}$ are functions of radial position only:

$$\delta\left(\frac{2}{3}\frac{J_{\|}^{2}}{\sigma_{\|}} + \varphi(T_e)\right) = \frac{4}{3}\frac{J_{\|}}{\sigma_{\|}}\,\delta(\underset{\sim}{hh}\cdot\underset{\sim}{J}) - \frac{2}{3}\frac{J_{\|}^{2}}{\sigma_{\|}}\frac{\delta\sigma_{\|}}{\sigma_{\|}} + \frac{\partial\varphi}{\partial T_e}\,\delta T_e$$

or,

$$\delta\left(\frac{2}{3}\frac{J_{\|}^{2}}{\sigma_{\|}} + \varphi(T_e)\right)\underset{\sim}{hh}\cdot\underset{\sim}{J} = P_e\left(\frac{4}{3}\,\omega_{OH}\left(\frac{\delta J_{\|}}{J_{\|}} + \frac{J_y}{J_{\|}}\frac{\delta B_y}{B}\right) - \left(\omega_{OH} - \frac{1}{n}\frac{\partial\varphi}{\partial T_e}\right)\frac{\delta T_e}{T_e}\right) \quad , \quad (A1)$$

where ω_{OH} is the ohmic heating rate $J_{\|}^{2}/\sigma_{\|}P_e$. In our model we assume long resistive diffusion time scales that lead to a close balance of ohmic heating and radiation losses rates in the equilibrium configuration. Under this assumption, the last term in Eq. (A1) should stay close to zero and we shall neglect its contribution:

$$\delta\left(\frac{2}{3}\,\nabla\cdot(\chi_{\parallel}^{e}\underset{\sim}{hh}\cdot\nabla T_e)\right) = \frac{2}{3}\,\nabla\cdot\left(\chi_{\parallel}^{e}\underset{\sim}{h}\delta(\underset{\sim}{h}\cdot\nabla T_e)\right) = \frac{2}{3}\,\underset{\sim}{h}\cdot\nabla\left(\chi_{\parallel}^{e}\delta(\underset{\sim}{h}\cdot\nabla T_e)\right)$$

$$= \frac{2}{3}\,i\,k_{\parallel}\chi_{\parallel}^{e}\,\delta(\underset{\sim}{h}\cdot\nabla T_e) = \frac{2}{3}\,i\,k_{\parallel}\chi_{\parallel}^{e}\left(i\,k_{\parallel}\,\frac{\delta T_e}{T_e} + \frac{dT_e}{dr}\,\frac{\delta B_r}{B}\right) ,$$

or in terms of the electron thermal conductivity,

$$\delta\left(\frac{2}{3}\,\nabla\cdot(\chi_{\parallel}^{e}\underset{\sim}{hh}\cdot\nabla T_e)\right) = P_e\omega_{CD}\left(i\,\frac{d\ell nT_e}{k_{\parallel}dr}\,\frac{\delta B_r}{B} - \frac{\delta P_e}{P_e} + \frac{\delta n}{n}\right) . \qquad (A2)$$

We proceed by presenting the expanded version of the heat drift flux [third term in Eq. (10)]:

$$\delta\left(\frac{5}{3}\,\nabla\cdot\left(\frac{cP_e}{eB}\,\underset{\sim}{h}\times\nabla T_e\right)\right) = \frac{5}{3}\,i\xi\,P_e\,V\left[\left(\frac{d\ell nB}{dr} - \frac{d\ell nn}{dr}\right)\frac{\delta P_e}{P_e} - \left(\frac{d\ell nB}{dr} - \frac{d\ell nP_e}{dr}\right)\frac{\delta n}{n}\right.$$

$$\left. - \frac{d\ell nT_e}{k_y dr}\left(\left(1 - \frac{k_{\parallel}^2}{k_y^2}\right)\frac{\delta B_{\parallel}}{B} - \frac{k_{\parallel}}{k_y}\,\frac{k_r}{k_y}\,\frac{\delta B_r}{B}\right)\right] . \qquad (A3)$$

Finally, the combined expression for the thermal force effect and the heat generated by the relative parallel flow of the species [last term in Eq. (10)] can be linearized:

$$\delta\left(\frac{2}{3}\,\tau\,\frac{T_e}{e}\,\nabla\cdot\underset{\sim}{J}_{\parallel}\right) = \frac{2}{3}\,\tau\,\frac{T_e}{e}\,\nabla\cdot\left(\delta(\underset{\sim}{hh}\cdot\underset{\sim}{J})\right)$$

$$= \frac{2}{3}\,i\tau\,P_e\frac{k_{\parallel}J_{\parallel}}{e\,n}\left(\frac{\delta J_{\parallel}}{J_{\parallel}} + \frac{J_y}{J_{\parallel}}\,\frac{\delta B_y}{B} - \frac{\delta B_{\parallel}}{B}\right) . \qquad (A4)$$

If we sum up Eqs. (A1)–(A4), divide by P_e, and separate the coefficients of $\delta P_e/P_e$ and $\delta n/n$, we obtain:

$$Q_p = Q_1 - \frac{5}{3}\, i\xi\, V\, \frac{d\ell nn}{dr} + \beta_e\, Q_o \tag{A5}$$

and

$$Q_n = -Q_1 - \frac{5}{3}\, i\xi\, V\, \frac{d\ell nP_e}{dr} + \beta_i\, Q_o \quad , \tag{A6}$$

where

$$Q_o = \frac{1}{3}\left(\frac{\underset{\sim}{k}\cdot\underset{\sim}{J}}{k_\parallel J_\parallel}\, Z_\parallel (2\,\omega_{OH} + i\,\tau\,\frac{k_\parallel J_\parallel}{en} + \frac{1}{2}\, Q_2\right) \quad , \tag{A7}$$

$$Q_1 = -\omega_{OH} - \omega_{CD} + \frac{5}{3}\, i\xi\, V\, \frac{d\ell nB}{k_y dr} \quad , \tag{A8}$$

and

$$Q_2 = \frac{4}{3}\,\omega_{OH}\,\frac{J_y}{J_\parallel}\, Z_y + \frac{2}{3}\, i\,\tau\,\frac{k_\parallel J_\parallel}{en}\left(\frac{J_y}{J_\parallel}\, Z_y - Z_\parallel\right) + i\xi\,\frac{d\ell nT_e}{k_\parallel dr}\left[\omega_{CD}\, Z_r\right.$$

$$\left. + \frac{5}{3}\, V\left(k_\parallel\,\frac{k_r}{k_y}\, Z_r - \left(i - \frac{k_\parallel^2}{k_y^2}\right) Z_\parallel\right)\right] \quad . \tag{A9}$$

Notice that in the electrostatic approximation, all Z_s are taken equal to zero, in which case $Q_2 = 0$ and Q_ν attains the form presented in Eqs. (26)–(27) with $Q_T \equiv Q_p$ and $Q_n \equiv Q_p + Q_n$.

☆ U.S. GOVERNMENT PRINTING OFFICE: 1984-0-776-026/4065